Continuous zircon-type tetragonal $Y_xBi_{0.95-x}VO_4$: $0.05Dy^{3+}$ solid solution: synthesis, characterization, and optical properties

Juan Yi (易 娟)[1], Yu'an Wang (王宇岸)[2], Dacheng Zhou (周大成)[1], and Jianbei Qiu (邱建备)[1*]

[1]*School of Materials Science and Engineering, Kunming University of Science and Technology, Kunming 650093, China*

[2]*Shenzhen Water (Group) Co. Ltd, Shenzhen 518000, China*

[*]*Corresponding author: qiu@kmust.edu.cn*

Received March 30, 2014; accepted May 20, 2014; posted online August 22, 2014

We synthesize continuous solid solutions with monophasic zircon-type structure of vanadates of formula $Y_xBi_{0.95-x}VO_4$:$0.05Dy^{3+}$ ($x = 0$–0.95) using a combined method of co-precipitation and hydrothermal synthesis. The X-ray diffractometer patterns confirm the formation of a solid solution of $Y_xBi_{0.95-x}VO_4$:$0.05Dy^{3+}$, and the results show that all the samples have monophasic zircon-type structure. The absorption spectra of the prepared phosphors show a blue-shift of the fundamental absorption band edge with increasing Y^{3+} content. An intense tunable characteristic emission of Dy^{3+} is observed with the increasing ratio of Y/Bi. Finally, the mechanism of luminescence of Dy^{3+} in the $Y_xBi_{0.95-x}VO_4$:$0.05Dy^{3+}$ ($x = 0$–0.95) solid solution is analyzed and discussed.

OCIS codes: 160.0160,230.0230,300.0300.

doi: 10.3788/COL201412.091601.

White light-emitting diode (W-LED) is one of the most potential candidates for solid-state lighting sources in the lighting industry[1,2]. At present, W-LEDs are usually fabricated by combining a blue LED chip with a yellow phosphor ($YAG:Ce^{3+}$)[3,4]. However, the present technical bottleneck is that the as-resulted white light has poor color rendering index because of color deficiency in the red region[5]. Moreover, the excitation range of most current phosphors is exceedingly narrow, resulting in the suitableness for only a few LED chips. To improve the properties of W-LEDs, several methods have been adopted. One strategy is to explore a novel long-wavelength yellow phosphor and to develop novel host materials with adjustable band gap, in order to suit for different LED chips. It is well known that Dy^{3+} ion has two intense fluorescence transitions from the $^4F_{9/2} \rightarrow {}^6H_{15/2}$ and $^4F_{9/2} \rightarrow {}^6H_{13/2}$ levels with the blue light emission at 480 nm and yellow light emission at 575 nm, respectively. Thus, white light can be obtained from Dy^{3+} activated materials by either changing the intensity ratio of the blue to yellow emissions or by adjusting the host composition[6].

Recently, the interest in solid-state materials of vanadium oxide doped with rare-earth ion has significantly grown because of their long-wavelength properties and excellent chemical stabilities[7]. Among the vanadium oxide, bismuth vanadate and yttrium vanadate are useful phosphors in observing different visible (Vis) colors with the suitable dopant rare-earth ions[8]. $BiVO_4$ can crystallize in three main structures (orthorhombic pucherite, tetragonal zircon, and monoclinic clinobisvanite), and vanadates with tetragonal zircon structure are considered as good host lattice under near-ultraviolet (UV) or blue excitation due to its tetrahedron unit. Unfortunately, the intensity of $BiVO_4$ or YVO_4 doped rare-earth emission is weaker than commercial phosphors. In this work, we attempted to construct a $BiVO_4$–YVO_4 solid solution to solve this problem. The formation of the $BiVO_4$–YVO_4 solid solution widens the band gap of $BiVO_4$ and enhances the intensity of emission light[9]. While the band gap of YVO_4 lies in the near-UV range (3.5 eV), that of $BiVO_4$ lies at the edge of the Vis range (2.9 eV) and depending on these band gaps, the band gap of the solid solution can be adjusted by changing yttrium content. Thus, zircon-type YVO_4 is a very ideal candidate material with $BiVO_4$ for constructing $Y_xBi_{0.95-x}VO_4$:$0.05Dy^{3+}$ solid solution.

To the best of our knowledge, there has been no report on the fabrication and optical properties for completed $BiVO_4$-based solid solution with monophasic zircon-type tetragonal, which use the traditional synthesis methods and these traditional synthesis methods need high calcination temperature or long synthesis time. Furthermore, the biphase mixture of tetragonal phase and monoclinic phase were obtained using single preparation process. Therefore, a new synthesis strategy combined with co-precipitation and hydrothermal methods was addressed. Based on the progress mentioned above, the initial purpose of this letter is to investigate whether the $Y_xBi_{0.95-x}VO_4$:$0.05Dy^{3+}$ binary system forms a complete solid solution with the monophase zircon structure. Then, the crystalline structure and the optical properties of $Y_xBi_{0.95-x}VO_4$:$0.05Dy^{3+}$ solid solution have been characterized and analyzed.

Analytical reagent grade NH_4VO_3, $Bi(NO_3)_3 \cdot 5H_2O$, Y_2O_3, Dy_2O_3 were employed as raw materials, which were weighed out and were added to nitric acid solution and dissolved with stirring at room temperature, then mixed homogeneously. The solution pH was adjusted to 2 with ammonia solution. The suspension was transferred into a 100 mL Teflon-lined stainless steel autoclave, and the hydrothermal treatment was carried out at 180 ℃ for 6 h. After the reaction suspension was carried out, centrifuged, and dried, the powder samples were obtained.

The crystal structures of phosphor samples were characterized by X-ray diffractometer (XRD, Cu-Kα: $\lambda = 0.1542$ nm, D8 Advance, German). The optical properties of absorption were measured by UV-Vis diffuse reflectance spectrophotometer (UV-Vis DR, Hitachi U-4100, Japan), and the photoluminescence (PL) spectra, including emission and excitation spectra, was obtained using a spectrophotometer equipped with InGaAs as detector with both continuous and pulsed xenon lamps (150 W, Hitachi F7000, Japan). All the measurements were carried out at room temperature.

The XRD patterns of the vanadate-based $Y_xBi_{0.95-x}VO_4$:0.05Dy^{3+} ($0 \le x \le 0.95$) phosphors are presented in Fig. 1 with a different Bi/Y ratio. $BiVO_4$ has a zircon-type structure with space group of $I4_1/amd$, which is identical with the YVO_4. The XRD patterns of the powder samples show that the phase in the powder samples matches well with the tetragonal structure of usual zircon-type of $BiVO_4$ or YVO_4, indicating that the phase in these phosphors are completed monophasic zircon-type structure combined with co-precipitation and hydrothermal methods. With the increase in Y^{3+} ions content, the position of main diffracted peak of the samples continuously shifts toward larger angles. The successive shift of the XRD pattern indicates that the lattice parameter decrease and the crystals obtained are not mixtures of $BiVO_4$ and YVO_4 phases, but $Y_xBi_{0.95-x}VO_4$:0.05Dy^{3+} solid solution. The ionic radius of the Y^{3+} ion for the coordination number (CN) six is 0.090 nm which is very close to that of Bi^{3+} (0.103 nm). It can be clearly seen that the ionic radius difference is less than the 15% limit stated by Vegard's law to achieve complete solid solubility between the dopant and the host cation. Therefore, the Y^{3+} ions are expected to occupy the Bi sites in these phosphors.

Figure 2 shows the UV-Vis absorption spectra of the $Y_xBi_{0.95-x}VO_4$:0.05Dy^{3+} powder samples at room temperature. The absorption spectrum of the pure $BiVO_4$ and YVO_4 are in agreement with that synthesized by an aqueous process reported before[10,11]. Semiconductors absorb light below a threshold wavelength λ_g, the fundamental absorption edge, which is related to the band gap energy via[12]

$$\lambda_g\,(\text{nm}) = 1240/E_g\,(\text{eV}).$$

The onset wavelengths of the absorption spectrum indicated that the band gaps of $BiVO_4$ and YVO_4 are 2.9 and 3.5 eV, respectively. We can see that the absorption edges of solid solutions $Y_xBi_{0.95-x}VO_4$:0.05Dy^{3+} are located between those of $BiVO_4$ (~430 nm) and YVO_4 (~360 nm). The absorption bands of solid solutions gradually shift to shorter wavelengths due to the increasing ratio of bismuth to yttrium in the solid solution. The phenomena should be attributed to a band transition of $Y_xBi_{0.95-x}VO_4$:0.05Dy^{3+} solid solution. This shift also indicates that the crystals obtained are solid solutions. To the best of our knowledge, the physical properties of continuous solid solution changes continuously with the composition. According to this principle, the formulation of continuous solid solution could be determined. The band gaps of $Y_xBi_{0.95-x}VO_4$:0.05Dy^{3+} solid solutions are estimated to be 2.9–3.5 eV from onsets of the absorption spectra. In other words, the formation of the solid solution widens the band gap

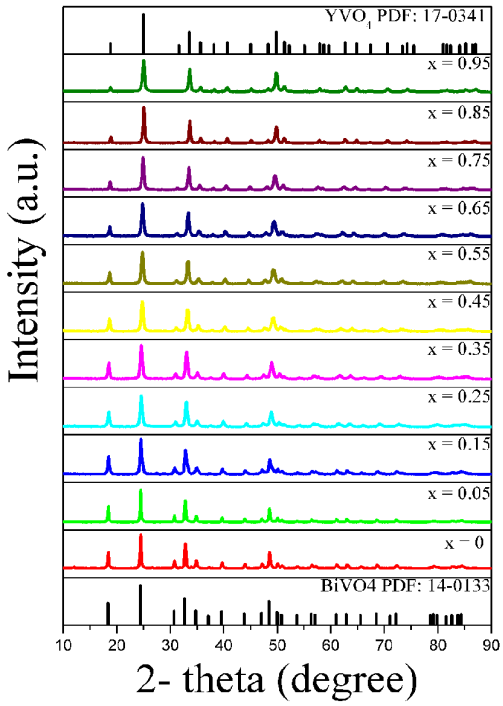

Fig. 1. XRD patterns of $Y_xBi_{0.95-x}VO_4$:0.05Dy^{3+} solid solutions ($0 \le x \le 0.95$).

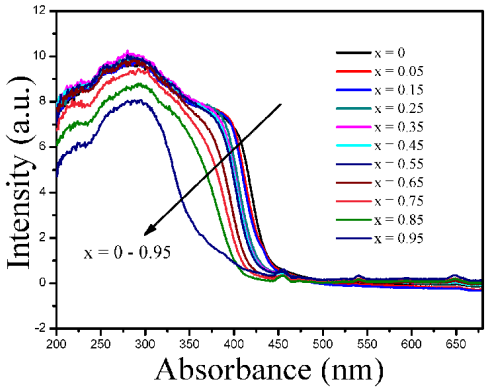

Fig. 2. UV-Vis absorption spectrum of $Y_xBi_{0.95-x}VO_4$:0.05Dy^{3+} ($x = 0$~0.95) solid solution.

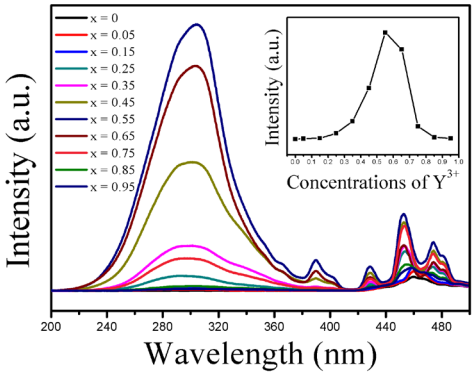

Fig. 3. Room temperature excitation spectra of $Y_xBi_{0.95-x}VO_4$:0.05Dy^{3+} (x = 0–0.95) solid solution (λ_{em} = 574 nm).

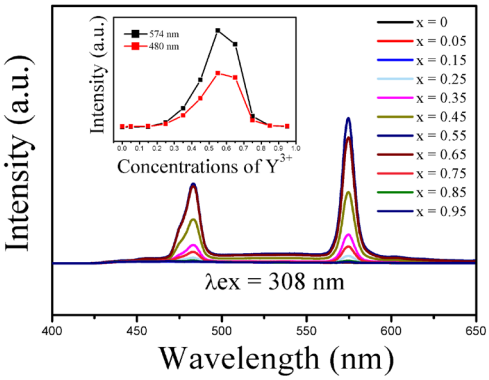

Fig. 4. Room temperature emission spectra of $Y_xBi_{0.95-x}VO_4$:0.05Dy^{3+} (x = 0–0.95) solid solution (λ_{ex} = 308 nm).

of $BiVO_4$, which can be reasonably understood, considering the larger band gap of YVO_4. Thus, the band gap of the $Y_xBi_{0.95-x}VO_4$:0.05Dy^{3+} solid solutions are controlled by the change in Bi/Y ratio in the composition. These imply that the band gap of $Y_xBi_{0.95-x}VO_4$:0.05Dy^{3+} ($0 \le x \le 0.95$) solid solutions could be adjusted and controlled by changing the value of x, all of the samples are tetragonal structure, which is its most important feature.

For Dy^{3+}-doped samples, the excitation spectra monitored at 574 nm are shown in Fig. 3. The PL excitation spectrum of $Y_xBi_{0.95-x}VO_4$:0.05Dy^{3+} ($0 \le x < 0.95$) shows a broad excitation band centered at 308 nm with a band edge at about 350 nm, the excitation band might be caused by the transition between the Bi^{3+} ions and the host lattices, instead of the conventional 6s → 6p transition ($^1S_0 \rightarrow {}^3P_1$) of Bi^{3+}. Blass *et al.*[13] demonstrated that for the Bi^{3+} doped YVO_4, the 6s level of Bi^{3+} lied above the highest filled 2p level of O^{2-}, thus the electrons in the 6s level were apt to be transferred to the 3d level of V^{5+}. Similarly, the 308 nm excitation band herein might be ascribed to the metal–metal (Bi^{3+}–V^{5+}) charge transfer followed by energy transfer to Dy^{3+}. Noticeably, the dominant energy transfer to Dy^{3+} with the ratio of bismuth to yttrium in the solid solution increased which is a charge transfer band which arises from the oxygen ligands interaction with the central metal ions (VO_4^{3-}(V–O)) components of the matrix[14]. It can be ascribed to the $^1A_1$–$^1T_1$ transition of VO_4^{3-}[15]. There are some sharp lines in the longer wavelength region, they are ascribed to the f–f transitions within Dy^{3+} $4f^9$ configuration. This suggests that, the solid-solution phosphors could enhance the near-UV LED chip excitation for obtaining the characteristic emissions.

The luminescence spectra of Dy^{3+}-doped $BiVO_4$-YVO_4 as-synthesized phosphors are shown in Fig. 4. The emission spectrum shows similar trend for all as-prepared phosphors. The spectral peaks at 480 nm (blue color) and 574 nm (yellow color) corresponding to $^4F_{9/2} \rightarrow {}^6H_{15/2}$ and $^4F_{9/2} \rightarrow {}^6H_{13/2}$ emission transitions of Dy^{3+} have been observed, dominated by the Dy^{3+} $^4F_{9/2} \rightarrow {}^6H_{13/2}$ hypersensitive transition ($\Delta J = 2$). This is because the Dy^{3+} is located at a low symmetry local site (D_{2d}, without inversion center) in the host lattices[11]. The $^4F_{9/2} \rightarrow {}^6H_{15/2}$ transition is magnetically allowed and hardly varies with the crystal field strength around the dysprosium ion. The presence of the VO_4^{3-} absorption in the excitation spectrum of Dy^{3+} indicates that an energy transfer occurs from VO_4^{3-} to Dy^{3+} in $Y_xBi_{0.95-x}VO_4$:0.05Dy^{3+} solid solution, and the energy transfer is very efficient because the emission of Dy^{3+} is observed upon excitation at the VO_4^{3-}. Moreover, it is also clear that the luminescent intensity highly depends on the solid solubility. It is observed from the inset that the Dy^{3+} emission intensifies with the increase in Y^{3+} content from 0 to 0.55; however, it turns to be weakened when Y^{3+} content exceeds 55 mol%. One main possibility of the phenomenon on the $Y_xBi_{0.95-x}VO_4$:0.05Dy^{3+} ($0 \le x \le 0.95$) systems can be analyzed. Theoretically, if the ions are far separated from each other, the energy transfer is not efficient. On the other hand, the closely spaced ions will lead to deleterious cross-relaxation, which decreases the emission efficiency[12]. Thus, the fluorescence emission of the solid-solution samples are affected by the distance between emission centers Dy^{3+} and VO_4^{3-}. The Y^{3+} ion is carefully chosen to have an ionic size slightly smaller than Bi^{3+} to make replacement of Bi^{3+} with the ion possible. The purpose of Y^{3+} ion doping is to slightly change the volume of the unit cell in the crystal and then improve the energy transfer efficiency to Dy^{3+} ion, and eventually increase the fluorescence emission. When a small amount of Y^{3+} ion is doped, they may occupy the lattice sites. The crystal unit cell will diminish only when it occupies the lattice sites[16]. Then comparing the XRD pattern in Fig. 1 with standard PDF card 014-0133, it is found that all the diffraction peaks slightly shifted to large diffraction angles, suggesting that the volume of unit cell shrinks after the Y^{3+} ions doping. The increase in PL intensity up to x = 0.55 may be caused by the fact that the solid solution with proper crystal unit cell efficiently

absorbed the excitation energy and transferred it to the Dy^{3+} activator. When the amount of the Y^{3+} ion is further increased, the decrease in emission intensity may be due to extreme shrinking of the unit cell, which causes the distances between emission centers Dy^{3+} and VO_4^{3-} become closer, and quenching might occur. We believe that quenching is caused by energy transfer among activators, that is, energy transfer occurs from one activator to another until an energy sink in the lattice is reached. Thus, energy transfer should be very sensitive with the concentrations. Besides, small particles do not have high luminous efficiency due to grain boundary effects[17]. Therefore, this is an indication that certain properties of the solid solution, such as crystallite size or disorder of the local environment surrounding the activator ions, influenced the PL spectra and the solid solubility is important to extract the maximum luminous efficiency.

The zircon-type tetragonal of $BiVO_4$ and YVO_4 crystals has a direct optical band gap. The gap between the lowest energy of the conduction band and the highest energy of the valence band are about 2.9 and 3.5 eV, respectively. The possible energy transfer processes are shown in Fig. 5. As shown in Fig. 5 ($x = 0$), under excitation at 308 nm, the electron of the $BiVO_4$:Dy^{3+} crystal absorbs energy and transits from the highest of the valence band to the conduction band. The Dy^{3+} ions first populate the lower $^4F_{9/2}$ level from the upper $^4I_{15/2}$ level via non-radiative transition, then return to the ground state with diverse probabilities and radiate the $^4F_{9/2}$–$^6H_{13/2}$ and $^4F_{9/2}$–$^6H_{15/2}$ emissions. Instead of transferring energy to Dy^{3+}, the energy may be relaxed to the ground state of the VO_4^{3-} group directly. But the relaxation process is less efficient than the transition process in this case; the emission peak of VO_4^{3-} is hard to find. However, for the $Y_{0.55}Bi_{0.4}Dy_{0.05}VO_4$, when being

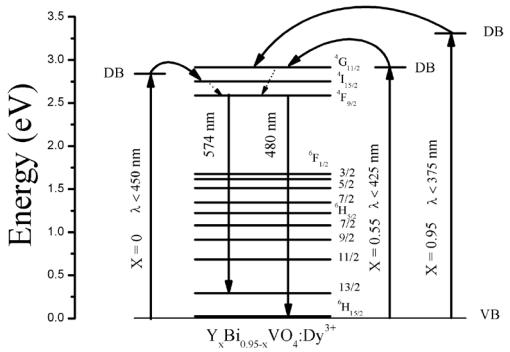

Fig. 5. Schematic diagram of energy levels of Dy^{3+} ion in $Y_xBi_{0.95-x}VO_4$:$0.05Dy^{3+}$ crystal as well as possible energy transfer processes.

excited at 308 nm, the lowest of the conduction band is matching in the $^4G_{11/2}$ level of Dy^{3+}, the intrinsic emission of Dy^{3+} is very intense. It indicates that the observed intense light emission in Fig. 4 is probably due to the high-efficient energy transfer transition from the host to Dy^{3+}. For the solid solution to achieve the purpose, the band gap can be adjusted and controlled by changing the value of x, then to tune the emission spectra intensity, it accounts for the excellent luminescence.

We discover from Fig. 4 that the intensity ratio of yellow-to-blue (Y/B) is strongly influenced by the value of x in the system of $Y_xBi_{0.95-x}VO_4$:$0.05Dy^{3+}$. Moreover, it is also clear that the shift of the emission color of the phosphor has been observed from blue-white to yellow region (Table 1 and Fig. 6). Surprisingly, the light is within the white region with a CIE coordinate of $x = 0.3032$ and $y = 0.3488$. In view of the above systematic investigations and by studying the effect of host composition (Bi, Y), it is seen that the

Table 1 CIE Coordinates of $Y_xBi_{0.95-x}VO_4$:$0.05Dy^{3+}$ Phosphors

x Value	CIE Chromaticity Coordinate		Emission Color
	x	y	
0	0.2426	0.2796	Bluish
0.05	0.2472	0.2901	Bluish
0.15	0.2537	0.2968	Bluish
0.25	0.277	0.3177	Bluish white
0.35	0.324	0.3788	Yellowish white
0.45	0.3418	0.4127	Yellowish
0.55	0.355	0.4271	Yellow
0.65	0.3473	0.4212	Yellowish
0.75	0.3032	0.3488	White
0.85	0.2527	0.2892	Bluish
0.95	0.2475	0.2862	Blue

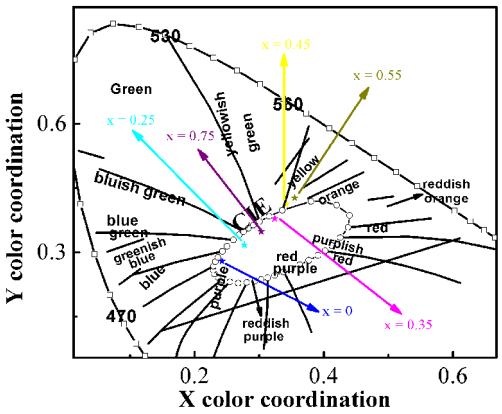

Fig. 6. Representation of the CIE chromaticity coordinates for $Y_xBi_{0.95-x}VO_4$:0.05Dy^{3+} phosphors upon 308 nm excitation.

luminescence intensity of $Y_xBi_{0.95-x}VO_4$:0.05Dy^{3+} phosphor is improved significantly. Thus, the phosphor with $Y_xBi_{0.95-x}VO_4$:0.05Dy^{3+} composition is finely tuned for enhanced long-wavelength yellow emission for its suitable application in certain optical display devices or lighting.

In conclusion, we successfully synthesize a monophasic zircon-type $Y_xBi_{0.95-x}VO_4$:0.05Dy^{3+} ($0 < x < 1$) solid solution by combining with co-precipitation and hydrothermal methods. XRD measurements reveal that the produced phosphors are good crystallines with pure phase and possess zircon-type tetragonal structure. Based on the results of UV-Vis absorption characterization, we find that the band gap of $Y_xBi_{0.95-x}VO_4$:0.05Dy^{3+} can be adjusted with Y^{3+} concentration. Emission peak intensities improve with the formulation of continuous solid solution. Especially, the emission intensity of $Y_xBi_{0.95-x}VO_4$:0.05Dy^{3+} ($x = 0.55$) is the strongest in all samples. Thus, $Y_xBi_{0.95-x}VO_4$:0.05Dy^{3+} is suggested as suitable yellow-emitting phosphor or W-LED.

This work was supported by the National 973 Program of China (No. 2011CB211708) and the National Natural Science Foundation of China (Nos. 51272097, 61265004, and 61307111).

References

1. L. Tang, H. Xia, P. Wang, J. Peng, and H. Jiang, Chin. Opt. Lett. **11,** 061603 (2013).
2. P. Xu, C. Xia, F. Wu, X. Li, Q. Sai, G. Zhou, and X. Xu, Chin. Opt. Lett. **10,** 021601 (2012).
3. S. Nakamura, MRS Bull. **22,** 29 (1997).
4. S. Nakamura and G. Fasol, *The Blue Laser Diode: GaN Based Light Emitters and Lasers* (Springer, Berlin, 1997) p. 317.
5. P. L. Li, Y. S. Wang, S. L. Zhao, F. J. Zhang, and Z Xu, Chin. Phys. B **21,** 127804 (2012).
6. Q. Su, Z. Pei, L. Chi, H. Zhang, Z. Zhang, and F. Zou, J. Alloys Compounds **192,** 25 (1993).
7. Q. Zhang, C. Guo, C. Shi, S.-Z. Lü, J. Alloys Compounds **309,** 10 (2000).
8. Q. Wang, Y. Li, Z. Zeng, and S. Pang, J Nanopart Res. **14,** 1076 (2012).
9. S. Neeraj, N. Kijima, and A. K. Cheetham, Chem. Phys. Lett. **387,** 2 (2004).
10. S. Tokunaga, H. Kato, and A. Kudo, Chem. Mater. **13,** 4624 (2001).
11. Y. Wang, S. Wang, Z. Wu, W Li, and Y Ruan, J. Alloys Compounds **551,** 262 (2013).
12. A. Hagfeldt and M. Gratzel, Chem. Rev. **95,** 49 (1995).
13. G. Blasse and A. Bril, J. Chem. Phys. **48,** 217 (1968).
14. S. Neeraj, N. Kijima, and A. K. Chetham, Solid State Commun. **131,** 65 (2004).
15. M. Yu, J. Lin, Z. Zhang, J. Fu, S. Wang, H. J. Zhang, and Y. C. Han, Chem. Mater. **14,** 2224 (2002).
16. Q. Dou and Y. Zhang, ACS Publ. **27,** 13236 (2011).
17. J. S. Yoo and J. D. Lee, J. Appl. Phys. **81,** 2810 (1997).